

# Channel modeling for optical wireless communication through dense fog

Urachada Ketprom, Sermsak Jaruwatanadilok, Yasuo Kuga,  
Akira Ishimaru, and James A. Ritcey

*Department of Electrical Engineering, Box 352500,  
University of Washington, Seattle, Washington 98195-2500*

*uketprom@u.washington.edu; ykuga@u.washington.edu*

RECEIVED 15 MARCH 2005; REVISED 23 APRIL 2005;

ACCEPTED 24 APRIL 2005; PUBLISHED 17 MAY 2005

The modified vector radiative transfer equation is solved in the frequency domain to study the frequency response of the propagation channel. In the time domain, the impulse response is obtained by taking the inverse Fourier transform of the frequency response. The time-domain analysis investigates the effects of the receiver's field of view on reducing the bit error rate when there is intersymbol interference caused by the temporal spread of the received signal.

© 2005 Optical Society of America

*OCIS codes:* 030.5620, 290.1310.

## 1. Introduction

The optical wireless communication (OWC) system has attracted significant interest because it can solve the last mile problem in urban environments. The last mile problem is when Internet providers cannot connect the fiber optic cables to every household user because of the high installation costs. The only disadvantage of the OWC system is that its performance depends strongly on weather conditions. Fog and clouds scatter and absorb the optical signal, which causes transmission errors. Most previous studies consider only single-scattering effects and assume that the received signal has no intersymbol interference (ISI), which is true only for light-fog conditions [1, 2].

This paper analyzes the ON-OFF keying (OOK) modulated light transmission through dense fog by using vector radiative transfer (RT) theory. RT theory is based on the assumption of power conservation, and it is applicable for studying multiple-scattering effects. We solve the vector RT equation for a band-limited signal to obtain the specific intensity of a received signal in the frequency domain. The results show the frequency response of the channel. The Fourier transform of the frequency response is the impulse response that characterizes the fog channel in the time domain. To obtain the expected received signal, we convolve the impulse response with the transmitted signal. In the time-domain analysis, our received signal includes not only the coherent intensity but also the incoherent intensity. The incoherent intensity causes pulse spreading, which results in the ISI in the system. We will introduce a technique to obtain the appropriate transmission rate for specified fog conditions and also a technique to adjust a receiver's field of view (FOV) to study the possibility of improving the link performance.

## 2. Optical Wireless Communication System

The OWC system is composed of three basic elements: the transmitter, the atmospheric channel, and the receiver. This study considers intensity-modulation-direct-detection (IM-DD) linking by OOK modulation. The atmospheric channel is modeled with fog whose contents are primarily water. Fog particles are spherical in shape and have radii varying

between 0.01 and 15  $\mu\text{m}$ , depending on geographical location [3]. The distribution of particles throughout the channel is assumed to be uniform. The fog's size distribution from Ref. [4] is shown in Table 1.

The real part of the index of refraction is obtained from the index of refraction of water at 25°C, corresponding to the 800 nm wavelength [5]. The imaginary part is assumed to be one thousandth of the real part to simulate minimal absorption. It is possible to identify a fog condition with a visibility range and relate it to the optical attenuation by using the Kruse formula. However, this formula is inapplicable to fog because the wavelength dependence of fog is too small in the visible and infrared range [6]. Therefore it is necessary to specify a fog condition with a parameter that is more general than a visibility range. In our model, the parameter that indicates the thickness of fog is the optical depth. Optical depth generally indicates the average number of interactions that light will incur when propagating through a multiple-scatter channel. The optical depth  $\tau_0$  is defined as  $\tau_0 = \rho\sigma_t L$ , where  $\rho$  is the number density of fog particles,  $\sigma_t$  is the scattering cross section, and  $L$  is the distance at which fog particles reside. In this study, we specify the distance  $L$  to be 300 m and assume that fog covers the whole length of the communication distance. Based on Ref. [7], for transmission range 300 m with optical carrier of 670 nm wavelength, an optical depth of about 10 corresponds to a visibility of less than 200 m, and an optical depth of about 3 corresponds to a visibility of 200–1000 m. Although the wavelength in our model is 800 nm, this relationship offers a rough idea on how to relate optical depth to visibility. Our model simulates results for  $\tau_0 = 1, 5, \text{ and } 10$ .

**Table 1. Particle Size Distribution of Fog**

Diameter ( $\mu\text{m}$ )	0.4	0.6	0.7	1.4	2.0	3.6	5.4	8.0
Particles (no./ $\text{cm}^3$ )	3	10	40	50	7	1	9	2

$n_{\text{fog}} = 1.3289 + i0.00132$  at  $\lambda = 800$  nm.

### 3. Radiative Transfer Equation and Its Solutions

We use the numerical solutions of the RT equation to analyze the propagation channel characteristics. The complete derivation for the RT equations is shown in Refs. [8–11]. For the vector RT equation, the specific intensity is given by the  $4 \times 1$  modified Stokes vector defined as

$$I = [I_1 \ I_2 \ U \ V]^T = [\langle E_1 E_1^* \rangle \ \langle E_2 E_2^* \rangle \ 2\Re\langle E_1 E_2^* \rangle \ 2\Im\langle E_1 E_2^* \rangle]^T. \quad (1)$$

Each Stokes parameter in the modified Stokes vector depends on four parameters: frequency  $\omega$ , forward angle  $\mu = \cos \theta$ , azimuthal angle  $\varphi$ , and the optical distance  $\tau$ , defined by  $\tau = \rho\sigma_t z$ , in which  $z$  is the propagation distance. When  $z = L$ , which is the length of the slab of the random medium,  $\tau$  becomes the optical depth  $\tau_0$ . The solution of the RT equation can be separated into reduced (coherent) intensity and diffuse (incoherent) intensity. Reduced intensity does not contain the multiple-scattering effects, and the solution is given by

$$I_{ri}(\tau, \omega) = I_0 \exp(-\tau_0) \delta(\mu - 1) \delta(\varphi). \quad (2)$$

We assume that the transmitted wave has a left-hand circular (LHC) polarization, and the incident intensity is given by  $I_0 = [1/21/201]^T$ . The diffuse intensity can be calculated by

using the modified pulse vector RT equation,

$$\left[ \mu \frac{\partial}{\partial \tau} + 1 + (\mu - 1) i \frac{\omega' + \omega_m}{\tau_0} \right] I'_d(\omega, \tau, \mu, \varphi) = \int_0^{2\pi} \int_{-1}^1 S(\mu, \varphi, \mu', \varphi') I'_d(\omega', \tau, \mu', \varphi') d\mu' d\varphi' + F_0(\mu, \varphi) f(\omega', \tau) \exp(-\tau), \quad \text{for } 0 \leq \tau \leq \tau_0, \quad (3)$$

where  $\omega = \omega_m + \omega'$ ;  $\omega$  is the normalized angular frequency, and  $\omega_m$  is the normalized angular modulation frequency [11].  $F_0(\mu, \varphi)$  is the source term and is given by  $F_0(\mu, \varphi) = [S][I_0(\mu, \varphi)]$ , where  $[S]$  is a  $4 \times 4$  scattering matrix or Mueller matrix defined in Refs. [10] and [11]. We apply Mie theory to solve for the scattering matrix under the assumption that a fog particle has a spherical shape. The size parameter, index of refraction, and wavelength are given in Table 1. We assume that the diffuse intensity is created inside a fog layer and that there is no diffuse intensity entering from outside. With this boundary condition, the discrete ordinate method is used for solving Eq. (3). Because the incident intensity has LHC polarization, the copolarized intensity of the received signal is given by  $I_{llp} = (I_1 + I_2 + V)/2$ . The diffuse intensity or the incoherent intensity is strongly dependent on the scattering angle. In the case of small scattering angle  $\theta$ , the integrated intensity  $J_d$  calculated from the diffuse intensity becomes

$$J_d(\tau, \omega) = \int_{\mu=\cos \theta} \int_{\varphi} I_d(\tau, \mu, \varphi, \omega) d\mu d\varphi = \int_{\theta=0}^{\Delta\theta} \int_{\varphi=0}^{2\pi} I_d(\tau, \theta, \varphi, \omega) d\theta d\varphi. \quad (4)$$

We assume that the diffuse intensity is uniform within a small range of  $\Delta\theta$  and Eq. (4) can be reduced to

$$J_d(\tau, \omega) \approx I_d(\tau, \omega) \pi (\Delta\theta^2). \quad (5)$$

Total intensity  $J_{\text{total}}$  is defined as the combination of diffuse and reduced intensities.

$$J_{\text{total}}(\tau, \omega) = I_d(\tau, \omega) \pi (\Delta\theta^2) + I_{ri}(\tau, \omega) \exp(-\tau). \quad (6)$$

Note that  $\theta$  is the discrete scattering angle obtained from the Gauss quadrature method and that there exists one value of diffuse intensity for each scattering angle. In Section 4, for each calculated frequency, we derive the magnitude and phase of  $J_{\text{total}}$  to obtain a frequency response. We also describe the method to obtain the impulse response that is derived from taking the Fourier transform of the frequency response.

#### 4. Frequency Response and Impulse Response of the Channel

In classical communication theory, the channel can be characterized in both time and frequency domains. The frequency response represents the characteristics of the channel as a function of frequency shown in Fig. 1.

Figure 1(a) shows that the frequency response of the channel has the characteristic of a low pass filter. The phase of the fog channel displays nonlinear characteristics at low frequency, and it depends on the optical depth as shown in Fig. 1(b). The bandwidth is commonly defined at a  $-3$  dB frequency. The received signals of  $\tau_0 = 1$  and 5 are always higher than  $-3$  dB for the frequency range that we calculated. For the  $\tau_0 = 10$  case, the bandwidth is limited to 5 MHz or twice the frequency shown in Fig. 1(a).

From the frequency response, we can obtain the impulse response by using the inverse Fourier transform. Figure 2 illustrates the different effects of FOV on the impulse response of the channel for  $\tau_0 = 1$  and 10. The impulse response of the greater optical depth channel displays a larger tail effect. The intensity underneath this tail suffers from multiple scattering and arrives at a later time than the intensity that travels in a direct path. Figure

2(b) shows that the tail effect also depends on the receiver's FOV. The large-tail impulse response is the result of severe multiple-scattering effects, and it becomes more apparent as the FOV increases. The impulse response with a large tail will cause an ISI problem. Therefore there is a trade-off between an additional power and a signal distortion when selecting FOV. In Section 5 we evaluate the effect of a multiple-scatter channel for a signal with a 5 MHz modulation frequency and explain the effect of FOV on a received signal.

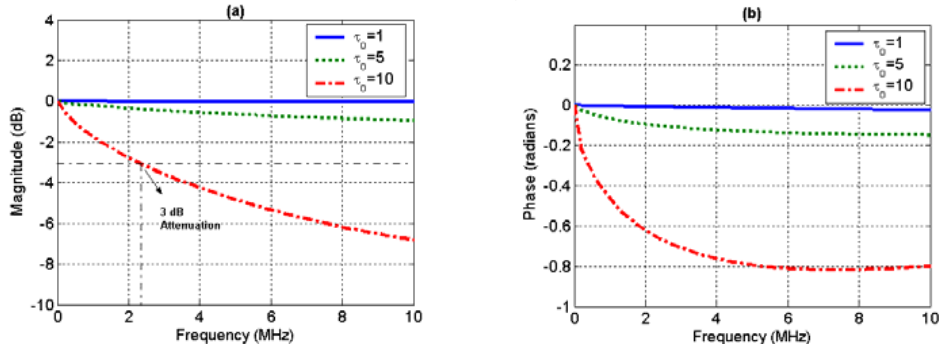


Fig. 1. Frequency response for optical depth = 1, 5, 10: (a) magnitude (b) phase.

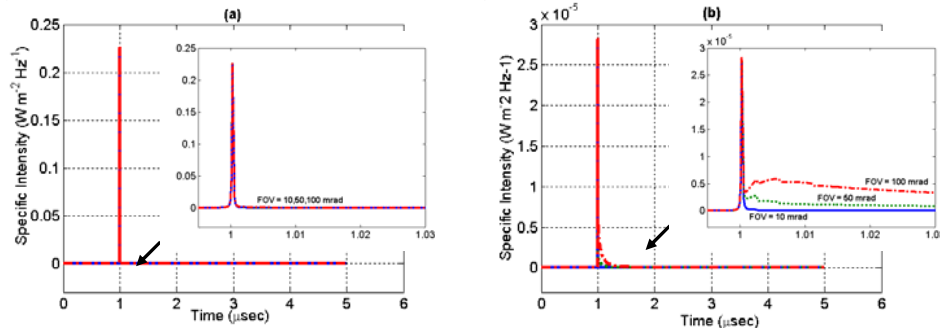


Fig. 2. Impulse response versus FOV: (a) optical depth= 1, (b) optical depth= 10.

## 5. Simulation of Received Signals

The expected received signal  $y(t)$  is the convolution of the transmitted signal  $x(t)$  and the impulse response of the fog channel  $h(t)$  plus the additive Gaussian noise  $n(t)$ , i.e. ,

$$y(t) = x(t) \otimes h(t) + n(t). \quad (7)$$

The transmitted signal  $x(t)$  is composed of nonreturn to zero (NRZ) bits with OOK format. The information bits are transmitted at a bit rate of  $R_b = 1/T$  bit/s, where  $T$  is the symbol period or symbol interval. The binary sequence emitted by the source is

$$z(t) = \sum_{n=-\infty}^{\infty} a_n g(t - nT), \quad (8)$$

where  $a_n$  (the information symbols) are binary random variables assuming the probability of  $\frac{1}{2}$  for the values of 0 and 1, and  $g(t)$  is the shaping pulse, normally a square pulse of

duration  $T'$ . Because we assume  $x(t)$  in NRZ, the pulse of duration  $T'$  is the same as the symbol period  $T$ .

In this section we focus on the multiple-scattering effect on the received signal without additional effects from system noises. The multiple-scattering effects cause the signal pulse to spread out. Figure 3(b) illustrates the pulse spread that induces the ISI when the scattering events are high in the channel. The wider FOV collects more light into the system; however, the ISI problem becomes worse. In Section 6 we show that the study of the bit-error-rate helps determine the correct FOV to optimize this trade-off.

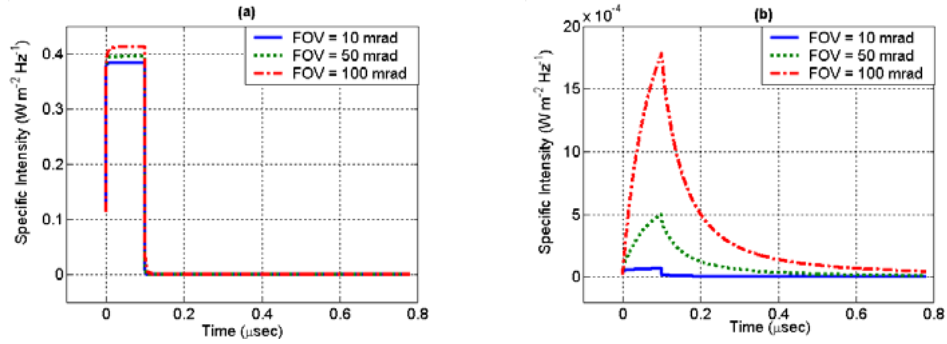


Fig. 3. Pulse response of 5 MHz signal: (a) optical depth = 1, (b) optical depth= 10.

## 6. System Performance with Noise Addition

### 6.A. Noise Consideration

Noise in the system depends on the characteristics of a receiver. A receiver is basically composed of photodetector and detection components. A photodetector changes the optical signal to an electrical signal. Detection components process and demodulate an electrical signal. We assume a simple OOK system with an integrate-and-dump receiver, so that the transmitter and receiver filters are identical and its behavior is similar to a bandpass filter. The optical signal with OOK encoding carries no negative power, but when optical signal is converted to an electrical signal, both DC and AC components occur. We assume that the DC component is filtered out before the detection process and that only the AC component undergoes maximum-likelihood detection.

In a detection process, we make two assumptions to avoid time extraction and AC coupling problems. First, we assume perfect time synchronization between transmitter and receiver. Second, we assume the DC components are perfectly extracted from the electrical signal after photodetection. Therefore the optimal decision threshold is half of the intensity from peak to peak of the AC component  $I_{AC}$ , i.e., zero. This study adopts the parameters for the PIN diode receiver model from Ref. [1]. We changed the receiver aperture diameter to be 20 cm instead of 10 cm because a larger aperture collects more light, which is necessary for communication in dense fog. The detector electronic bandwidth is also changed to 10 MHz, which is sufficient for the signal with 5 MHz modulation frequency propagating through dense fog. The parameters and values used are  $P_T$ , peak power (1 W);  $L$ , distance (300 m);  $T_F$ , filter transmissivity (0.5);  $\Delta\lambda$ , fiber optic bandwidth (10 nm);  $D_R$ , receiver aperture diameter (20 cm);  $\eta$ : P-I-N quantum efficiency (0.8);  $B$ , detector electronic bandwidth (10 MHz);  $R_L$ , load resistance (100  $\Omega$ );  $F$ , circuit noise figure (4);  $T_e$ , equivalent temperature (290 K); and  $H_{BKG}$ , background radiance (0.2 W m<sup>-2</sup> nm<sup>-1</sup> sr<sup>-1</sup>).

We also refer to the reduced intensity  $I_{ri}$  as the coherent intensity  $I_{coh}$  and refer to the diffuse intensity  $I_d$  as the incoherent intensity  $I_{inc}$ . The incoherent intensity  $I_{inc}$  is dependent on the scattering angle  $\theta$  as shown in Eq. (4). The FOV determines the amount of the integrated power from  $I_{inc}$  over the angles covered by the FOV, so  $I_{inc}$  depends on the FOV. When the FOV covers only one scattering angle  $\theta$ , we can interchange the half-angle FOV with the small scattering angle  $\Delta\theta$  in Eq. (5). However, when the FOV covers more than one scattering angle  $\theta$ , the integration of incoherent intensity from all scattering angles is required. The received power is calculated from the specific intensity obtained from the solution of the modified vector RT equation in Eq. (3), and it is normalized to the transmitted peak power of 1 W. The received power and background noise are defined as

$$P_s = J_{total}(\tau, \omega) A_r \Delta\lambda T_F = \left( I_{inc} \pi (FOV)^2 + I_{coh} (\exp(-\tau)) \right) A_r \Delta\lambda T_F, \quad (9)$$

$$P_{BG} = H_{BKG} \pi (FOV)^2 A_r \Delta\lambda T_F, \quad (10)$$

where  $A_r$  is the receiver area defined as  $A_r = \pi(D_R/2)^2$ . For noise consideration, the variances in detected current resulting from thermal noise, shot noise, and background radiation are defined as

$$\sigma_{TH}^2 = (4kT_eFB)/R_L, \quad \sigma_{ss}^2 = 2qRP_sB, \quad \sigma_{BG}^2 = 2qRP_{BG}B. \quad (11)$$

Responsivity (in amperes per watt) is used to characterize the efficiency of a photodiode in converting light to an electrical signal. It is defined as  $R = (\eta q \lambda) / (hc)$ , where  $\eta$  is the photodetector's quantum efficiency. The constants in Eq. (11) are Boltzmann's constant ( $k$ )  $1.381 \times 10^{-23}$ , Planck's constant ( $h$ )  $6.6 \times 10^{-34}$  J/s, the speed of light in free space ( $c$ )  $3.0 \times 10^8$  m/s, and electronic charge ( $q$ )  $1.6 \times 10^{-19}$  C.

Figure 4(a) displays the shot noise as a dominant noise when the optical depth equals 1. In this case the signal is rarely scattered by the fog particles. For the peak power transmission of 1 W, the shot noise induced by the signal is much more than the shot noise induced by background radiation. At optical depth 10, the signal is strongly scattered, and the shot noise induced by the signal is much less than both thermal and background noises. When the FOV is less than 200 mrad, the thermal noise is a dominant noise. Beyond this point, the background noise dominates other noises. The information on dominant noise helps determine the characteristics of the receiver and also simplifies the signal-to-noise ratio (SNR) equation in Subsection 6.B.

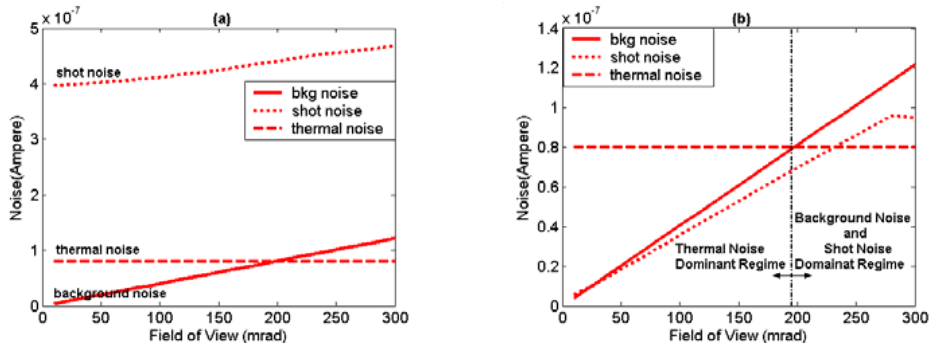


Fig. 4. Receiver noise versus FOV: (a) optical depth = 1, (b) optical depth= 10.

### 6.B. Signal-to-Noise Ratio Calculation

The received power during the ON state  $P_{sig1}$  is always higher than the received power during the OFF state  $P_{sig0}$ . The average received power  $P_s = P_{sig1} - P_{sig0}$  at the detector can be determined from the average intensity of received bits. These bits are the convolution results between the transmitting signal and the channel's impulse response. The SNR can be written as

$$\text{SNR} = \frac{R(P_{sig1} - P_{sig0})}{\sqrt{\sigma_0^2 + \sigma_1^2}}. \quad (12)$$

The detector current and noise variance due to received signal during the ON state are

$$I_1 = RP_{sig1} = RP_s + RP_{BG}, \quad \sigma_1^2 = \sigma_{ss}^2 + \sigma_{BG}^2 + \sigma_{TH}^2. \quad (13)$$

The detector current and noise variance due to received signal during the OFF state are

$$I_0 = RP_{sig0} = RP_{BG}, \quad \sigma_0^2 = \sigma_{BG}^2 + \sigma_{TH}^2. \quad (14)$$

Substituting Eqs. (13) and (14) into Eq. (12), we can write

$$\text{SNR} = \frac{RP_s}{\sqrt{\sigma_0^2 + \sigma_1^2}} = \frac{R \left( I_{coh} \exp(-\tau) + I_{inc} \pi (FOV)^2 \right) A_r \Delta \lambda T_F}{\sqrt{\sigma_{BG}^2 + \sigma_{TH}^2} + \sqrt{\sigma_{ss}^2 + \sigma_{BG}^2 + \sigma_{TH}^2}}. \quad (15)$$

While the coherent intensity is independent of the FOV, the incoherent intensity  $I_{inc}$  is affected by the FOV because it depends on the scattering angles that the FOV covers. When the optical depth equals 1, the incoherent intensity is much smaller than the coherent intensity; thus the FOV does not have much effect on the received signal, and the result in Fig. 5 displays an almost constant value of the SNR. For optical depth 10, the SNR increases when the FOV increases; however, there exists a limit for widening the FOV to increase the SNR. The limitation can be explained by Fig. 6, as the incoherent intensity approaches a constant at the large FOV values.

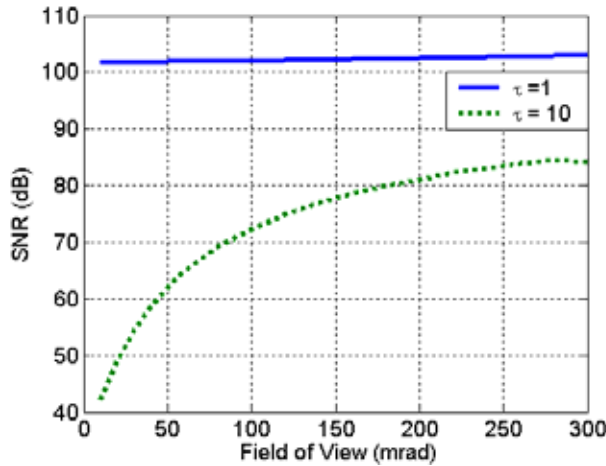


Fig. 5. SNR versus FOV.

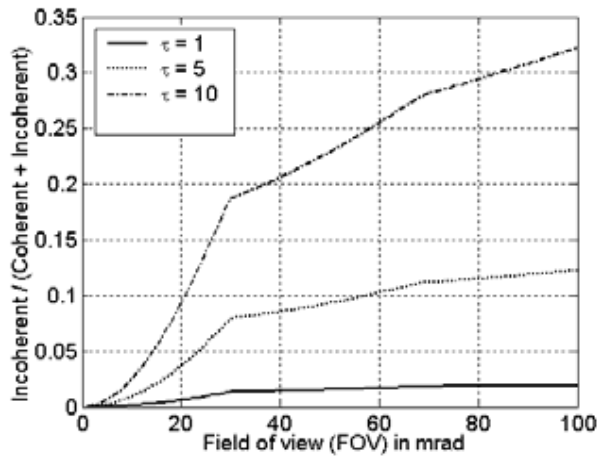


Fig. 6. Normalized incoherent intensity versus FOV.

### 6.C. Probability of Error

We perform a Monte Carlo simulation of bit transmission through a fog channel based on the impulse response method. The detection threshold of the receiver is determined from the average energy of the AC component of all received bits. The energy within each received bit is separately calculated and compared with the detection threshold. Any bit that has smaller energy than the detection threshold will be detected as “0,” and any bit that has larger energy will be detected as “1.” We divide the error bits by the total number of transmitted bits to obtain the probability of error or bit error rate.

For the specified system in our study, Fig. 7(a) shows that there is no error detected when the optical depth equals 1. As for the optical depth of 10, the probability of error decreases as the FOV increases when the FOV is smaller than 80 mrad. When the FOV is further increased in order to increase the SNR, the errors are no longer caused by the system noises but rather by the multiple-scattering effects that cause a pulse to spread. Figure 7(b) illustrates that the probability of errors approaches the minimum value determined by the channel condition when noise is negligible compared with signal. The minimum probability of error is 0.173 at an FOV of 80 mrad.

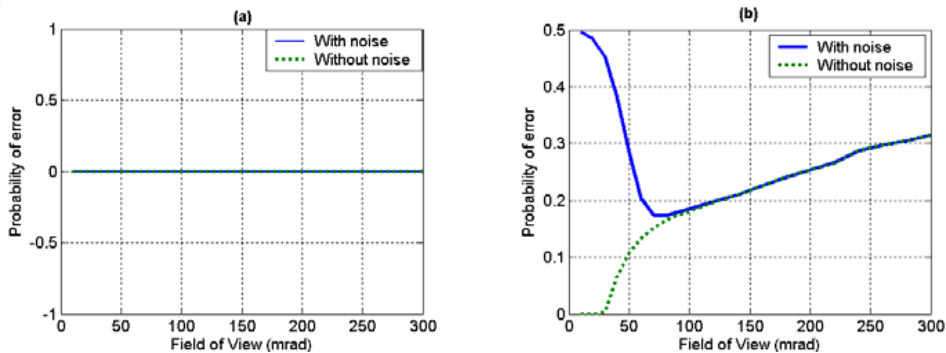


Fig. 7. Probability of error versus FOV: (a) optical depth = 1, (b) optical depth= 10.

Fog conditions must be considered when the FOV effect is studied. Our study covers two extreme cases: optical depth = 1 and = 10. In the light-fog condition (optical depth = 1), the FOV effect is very small because the coherent power completely dominates the incoherent power, and increasing FOV does not add much power to the received signal in this case. In the dense-fog condition (optical depth = 10), the incoherent power becomes comparable with the coherent power for a typical FOV of 50~100 mrad. The pulse shape of the signal is distorted from the large tail of the impulse response when FOV is enlarged to capture more light. For a large optical depth, the pulse spread that induces ISI causes errors so severe that the detector can no longer recognize the transmitted signal. When the wave distortion is significant, it is impossible to detect the correct bits even after adjusting the FOV to receive a better SNR.

## 7. Conclusions

We discuss the method to model the OWC communication links in dense-fog using RT theory. The impulse response of the channel convolved with the transmitted signals reveals the expected received signal in different fog conditions. We show that it is possible to increase SNR by widening FOV. This technique has no effect when shot noise is a dominant noise in a light-fog condition ( $\tau_0 = 1$ ). In a dense-fog condition ( $\tau_0 = 10$ ), the proposed technique is proved to be effective. We search for the optimal FOV, and the result shows that it is best to find the optimal FOV by considering the minimum bit error rate and not the maximum SNR when ISI is present in the system.

## Acknowledgment

This work is supported by the National Science Foundation (ECS-9908849), the Office of Naval Research (N00014-04-1-0074), and a Thai Government Scholarship.

## References and Links

- [1] H. Manor and S. Arnon, "Performance of an optical wireless communication system as a function of wavelength," *Appl. Opt.* **42**, 4285–4294 (2003).
- [2] B. R. Strickland, M. J. Lavan, E. Woodbridge, and V. Chan, "Effects of fog on the bit-error rate of a free-space laser communication system," *Appl. Opt.* **38**, 424–431 (1999).
- [3] S. Karp, R. M. Gagliardi, S. E. Moran, and L. B. Stotts, *Optical Channels: Fibers, Clouds, Water, and the Atmosphere (Applications of Communications Theory)* (Plenum, 1988).
- [4] National Institute for Resources and Environment, "Measurement of size distribution of aerosol by bistatic system" (NIRE, 2000), <http://www.aist.go.jp/NIRE/annual/1999/21.htm>.
- [5] G. M. Hale and M. R. Querry, "Optical-constants of water in 200-Nm to 200-Mum wavelength region," *Appl. Opt.* **12**, 555–563 (1973).
- [6] R. M. Pierce, J. Ramaprasad, and E. C. Eisenberg, "Optical attenuation in fog and clouds," in *Optical Wireless Communications IV*, E. J. Korevaar, Proc. SPIE 4530, pp. 58–71 (2001).
- [7] D. Kedar and S. Arnon, "Optical wireless communication through fog in the presence of pointing errors," *Appl. Opt.* **42**, 4946–4954 (2003).
- [8] S. Chandrasekhar, *Radiative Transfer* (Clarendon, 1950).
- [9] A. Ishimaru, *Wave Propagation and Scattering in Random Media* (IEEE, Oxford U. Press, 1997).
- [10] R. L.-T. Cheung and A. Ishimaru, "Transmission, backscattering, and depolarization of waves in randomly distributed spherical particles," *Appl. Opt.* **21**, 3792–3798 (1982).
- [11] S. Jaruwatanadilok, A. Ishimaru, and Y. Kuga, "Photon density wave for imaging through random media," *Waves Random Media* **12**, 351–364 (2002).